

Toward a precise localization of Zinc in InP crystal lattice using novel nondestructive approach of X-ray Standing Wave Technique

A. Ougazzaden¹, A.A. Sirenko², A. Kazimirov³

1) *Laboratoire Matériaux Optiques, Photonique et Systèmes, UMR CNRS 7132, Université de Metz and Supélec, 2, rue E. Belin, 57070 Metz, France*

2) *Department of Physics, New Jersey Institute of Technology, Newark, NJ 07102*

3) *Cornell High Energy Synchrotron Source (CHESS), Cornell University, Ithaca, NY 14853*

Precise control of the doping in the *p*-type semiconductor layers is important for fabrication of integrated optoelectronic structures. Zinc is a common *p*-type dopant used in InP-InGaAsP and InP-InGaAlAs systems grown by MOVPE. For example, Zn-doped InP with the carrier concentration more than 10^{18} cm^{-3} is widely used as *p*-type cladding layer on top of the adjacent undoped active region of the vast majority of InP-based optoelectronic *p-i-n* structures. Compared to other acceptors (Cd, Mg, and Be), Zinc has several crucial advantages, such as high solubility and low ionization energy, the latter results in relatively high degree of electrical activity of Zn at room temperature. However, the unintentional Zn diffusion during MOVPE growth is very fast compared to the *n*-type dopants. As a result, the Zn profile distribution, which has tremendous impact on the device characteristics, is hard to predict and control. For example, uncontrolled diffusion of Zn can displace the desired position of the *p-i-n* junction and change the build-in electric field in the active region of the device that usually deteriorates the performance at the high-speed. Extensive studies of InP and related materials resulted in a common agreement that Zn diffusion during the growth can be generally described by the substitutional-interstitial mechanism. Thus, interstitial zinc $\text{Zn}^{(i)+}$ diffuses until it is captured at the vacancies of the In-sublattice V_{In}^- to form substitutional zinc $\text{Zn}^{(s)-}$. The *p*-type carrier concentration is determined mostly by the substitutional fraction that behaves as a shallow acceptor, while the interstitial Zn does not contribute to the *p*-type carrier concentration and is not electrically active in this sense. In the attempt to suppress zinc diffusion keeping the conductivity and mobility of the InP layer at maximum, great care should be taken to control and minimize the interstitial fraction of Zn.

The standard approach to control Zn incorporation and activation in InP-based structures grown by MOVPE is an arrangement of Secondary Ion Mass Spectroscopy (SIMS) and electrochemical capacity-voltage (CV) profiling. However this combined indirect approach is destructive by its nature and it does not provide sufficient spatial resolution for *in situ* device structure characterization and the measurements has to be taken from the “control squares” of the device wafers. New nondestructive approaches for precise localization of *p*-type impurities in the *III-V* semiconductor matrix are required and a possibility to utilize such techniques at the micron-scale would be a big advantage for novel integrated optoelectronic devices.

In our recent experiments at the A2 beamline of CHESS we applied the nondestructive X-ray Standing Wave (XSW) technique to address incorporation of acceptor impurities in semiconductors [1]. Among investigated systems are Zn-doped InP, GaAs:Mn, Mg-doped and Er-doped GaN. Some of these measurements have been carried out with the in-plane spatial resolution of 10 μm using imaging capillary optics. In this paper we discuss the InP layers doped with Zn to the level of 10^{18} cm^{-3} grown epitaxially on InP (001) substrate and we also analyze the activation of Zn due to the post-growth rapid thermal annealing (RTA).

The X-ray Standing Wave (XSW) technique is based on the generation in and above the crystal the interference field emergent due to the superposition of the incident and Bragg-diffracted x-ray waves. The periodicity of the standing wave is the same as for the diffraction planes d_{hkl} . As the crystal is scanned through the Bragg peak, the standing wave field shifts inward by the half of its period $d_{hkl}/2$ in the direction normal to the diffraction planes. This movement modulates the interaction of the total electric field of the x-ray wave with atoms in the crystal lattice resulting in a pronounced angular dependence of the x-ray photoelectron absorption that can be observed by monitoring the fluorescence yields. In the first approximation, the angular dependence of the fluorescence yield $Y(\mathbf{q})$ from atoms of a diffracting crystal (In, P, and Zn) can be written as: $Y(\mathbf{q}) = 1 + R(\mathbf{q}) + 2f_H \cos(\mathbf{n}(\mathbf{q}) - 2\mathbf{p}P_H) \cdot \sqrt{R(\mathbf{q})}$, where $R(\mathbf{q})$ is the reflectivity, $\nu(\mathbf{q})$ is the phase of the

diffracted plane wave, and P_H and f_H are the phase and modulus of the H^{th} Fourier component of the atomic distribution function projected onto the crystal unit cell. Thus, measuring the fluorescence yield from doping atom one can determine its atomic position relative to the host unit cell [2,3]. The experimental data analysis based on the dynamic diffraction theory in layered crystals for several reflections (0 0 4, 1 1 1, 0 0 2, 0 0 6, and 0 2 2) can provide a clear 3D picture for distribution density of impurities, (*e.g.*, Zn) in semiconductor lattice (*e.g.*, InP).

Angular dependences of the Zn-K fluorescence excited by the XSW field inside the InP layer for symmetrical 0 0 4 and 0 0 2, as well as for non-coplanar 1 1 1 reflections have been measured along with the In-L and P-K fluorescence and X-ray reflectivity. The x-ray beam with the energy of 10 KeV produced by the synchrotron storage ring was utilized to excite fluorescence spectra in our samples. In general, fluorescence is dominated by the strong host-lattice signal related to In and P. The weak Zn-related $K\alpha_{1,2}$ fluorescence signal was integrated between 8.62 and 8.64 KeV. The experimental XSW curves for fluorescence yield from In and P host atoms and Zn acceptors are shown in Fig. 1 together with the x-ray reflectivity curve for 0 0 2 reflection of InP. The fluorescence yield curves for In and P have orthogonal phases, as it should be for the 0 0 2 reflection of ideal zinc-blend cubic crystal, when In and P atoms belong to the different d planes. Zn fluorescence repeats the main features of the In signal, as expected for acceptor impurities with a significant substitutional fraction. However, the observed deviation between In and Zn curves corresponds to the interstitial fraction of Zn. Analysis of the XSW data based on the dynamical diffraction theory in layered crystal structures allowed us to determine quantitatively the fractions of both the Zn atoms incorporated into crystal lattice and in the interstitial position, thus getting insight to the activation behavior of these important p -type dopant atoms.

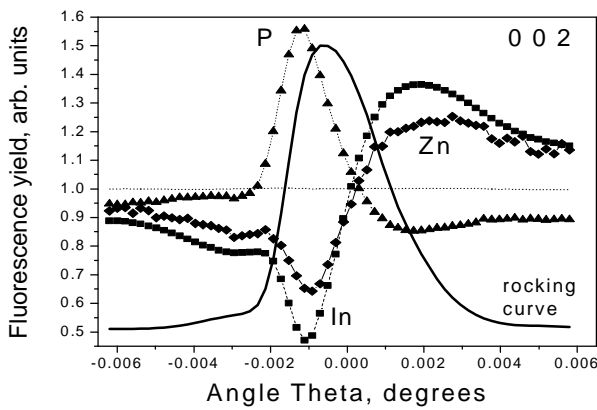


Fig. 1. Squares, triangles, and diamonds represent, respectively, fluorescence yield from In, P, and Zn atoms measured from the InP epilayer doped with Zn at the level of 10^{18} cm^{-3} . X-ray $\mathbf{q} - 2\mathbf{q}$ scan measured at the 0 0 2 reflection of InP is shown with a solid curve.

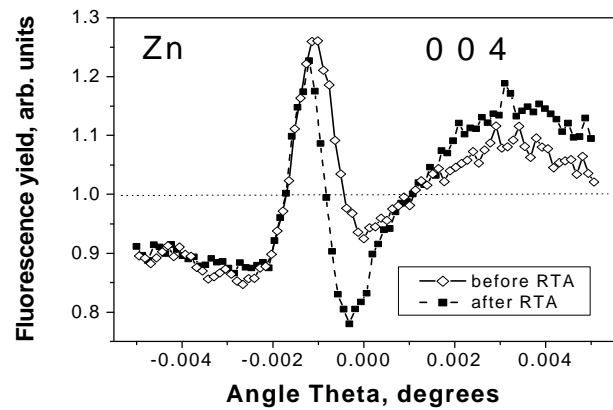


Fig. 2. Zn-related XSW signal measured at 0 0 4 reflection in the same InP sample before RTA (shown with open diamond) and after Rapid Thermal Annealing (RTA) at 600°C (shown with solid squares).

Figure 2 demonstrates the potential of the XSW technique to characterize the effect of the Rapid Thermal Annealing (RTA) on the activation of acceptor impurities. The nondestructively measured XSW experimental curves in Fig. 2 for 0 0 4 reflection have been compared to the calculated ones. In this sample, the coherent fraction of substitutional Zn has increased from the as-grown level of 64% up to 90% due to the RTA treatment at 600°C . This result has been confirmed by the SIMS and CV- profilometry data measured in the same sample before and after RTA.

References

- [1] A.A. Sirenko, A. Ougazzaden, and A. Kazimirov, Computational Materials Science **33**, 132 (2005).
- [2] B.W. Batterman, Phys. Rev. Lett. **22**, 703 (1969).
- [3] S.K. Andersen, J.A. Golovchenko, and G. Mair, Phys. Rev. Lett. **37**, 1141 (1976).